frontiers | Frontiers in Oncology

TYPE Original Research
PUBLISHED 11 September 2024
DOI 10.3389/fonc.2024.1417933

OPEN ACCESS

EDITED BY
Alessio G. Morganti,
University of Bologna, Italy

REVIEWED BY
Thomas Samuel Ram,
Christian Medical College and Hospital, India
Jingjing Zhang,
Wuhan University, China

*CORRESPONDENCE
Fenghai Liu
lfh600@126.com

RECEIVED 22 April 2024
ACCEPTED 21 August 2024
PUBLISHED 11 September 2024

CITATION
Xu X, Liu F, Zhao X, Wang C, Li D, Kang L, Liu S and Zhang X (2024) The value of multiparameter MRI of early cervical cancer combined with SCC-Ag in predicting its pelvic lymph node metastasis.
Front. Oncol. 14:1417933.
doi: 10.3389/fonc.2024.1417933

The value of multiparameter MRI of early cervical cancer combined with SCC-Ag in predicting its pelvic lymph node metastasis

Xiaoqian Xu[1], Fenghai Liu[1*], Xinru Zhao[1], Chao Wang[1], Da Li[1], Liqing Kang[1], Shikai Liu[2] and Xiaoling Zhang[3]

[1]Department of Magnetic Resonance Imaging, Cangzhou Central Hospital, Cangzhou, Hebei, China, [2]Department of Gynecology, Cangzhou Central Hospital, Cangzhou, Hebei, China, [3]Department of Pathology, Cangzhou Central Hospital, Cangzhou, Hebei, China

Purpose: To investigate the value of multiparameter MRI of early cervical cancer (ECC) combined with pre-treatment serum squamous cell carcinoma antigen (SCC-Ag) in predicting its pelvic lymph node metastasis (PLNM).

Material and methods: 115 patients with pathologically confirmed FIGO IB1~IIA2 cervical cancer were retrospectively included and divided into the PLNM group and the non-PLNM group according to pathological results. Quantitative parameters of the primary tumor include K^{trans}, K_{ep}, V_e from dynamic contrast-enhanced magnetic resonance imaging (DCE-MRI), ADC_{mean}, ADC_{min}, ADC_{max}, D, D* and f from intravoxel incoherent motion diffusion-weighted imaging (IVIM-DWI) were measured. Pre-treatment serum SCC-Ag was obtained. The difference of the above parameters between the two groups were compared using the student t-test or Mann-Whitney U test. Multivariate Logistic regression analysis was performed to determine independent risk factors. Receiver operating characteristic (ROC) curve analysis was used to assess the diagnostic efficacy of individual parameters and their combination in predicting PLNM from ECC.

Results: The PLNM group presented higher SCC-Ag [14.25 (6.74,36.75) ng/ml vs.2.13 (1.32,6.00) ng/ml, $P<0.001$] and lower K^{trans} (0.51 ± 0.20 min^{-1} vs.0.80 ± 0.33 min^{-1}, $P < 0.001$), ADC_{mean} (0.85 ± 0.09 mm/s^2 vs.1.06 ± 0.35 mm/s^2, $P<0.001$), ADC_{min} [0.67 (0.61,0.75) mm/s^2 vs. 0.75 (0.64,0.90) mm/s^2, $P = 0.012$] and f (0.91 ± 0.09 vs. 0.27 ± 0.14, $P = 0.001$) than the non-LNM group. Multivariate analysis showed that SCC-Ag (OR = 1.154, $P = 0.007$), K^{trans} (OR=0.003, $P < 0.001$) and f (OR = 0.001, $P=0.036$) were independent risk factors of PLNM. The combination of SCC-Ag, K^{trans} and f possessed the best predicting efficacy for PLNM with an area under curve (AUC) of 0.896, which is higher than any individual parameter: SCC-Ag (0.824), K^{trans} (0.797), and f (0.703). The sensitivity and specificity of the combination were 79.1% and 94.0%, respectively.

Conclusions: Quantitative parameters K^{trans} and f derived from DCE-MRI and IVIM-DWI of primary tumor and SCC-Ag have great value in predicting PLNM. The diagnostic efficacy of their combination has been further improved.

KEYWORDS

cervical cancer, magnetic resonance imaging, dynamic contrast-enhanced, intravoxel incoherent motion, diffusion-weighted imaging, squamous cell carcinoma antigen, lymph node metastasis

Introduction

Cervical cancer is one of the most common cancers and the fourth leading cause of cancer death in women worldwide (1). PLNM is a vital factor affecting the prognosis of cervical cancer (2), and the 5-year survival rate of patients with PLNM is significantly reduced (3). With the promotion of tumor screening, the proportion of ECC discovered has increased in recent years (4, 5). Radical hysterectomy with lymphadenectomy is the standard treatment for ECC according to FIGO guideline. However, the incidence of PLNM in ECC is less than 30% (6), most patients are over-treated, which increases the risk of surgery and may lead to complications. For ECC patients with PLNM, concurrent chemoradiotherapy is commonly recommend by ESMO clinical practice guideline, and there is no significant difference in survival and recurrence rates compared to surgical intervention (7, 8). Therefore, accurate preoperative assessment of pelvic lymph node status is crucial for optimizing the treatment plan of ECC and is also a difficult point in clinical practice.

MRI is currently the prior imaging method for non-invasive evaluation of PLNM. The differential efficacy of conventional MRI which based on morphologic features to diagnose PLNM is still limited due to the presence of inflammatory hyperplasia and micro metastatic lymph nodes (9). The emergence of functional MRI has made it possible to quantitatively analyze changes in the microenvironment of lesions, making up for the shortcomings of conventional MRI (10, 11). Diffusion weighted imaging (DWI) can provide information on tumor cell density and membrane integrity, making it a powerful auxiliary tool for distinguishing between benign and malignant lymph nodes (12). However, the single b-value DWI does not exclude the influence of microvascular perfusion, and there are limitations in the accuracy of its diffusion parameters (13). IVIM-DWI and DCE-MRI can truly reflect vascular permeability and microcirculatory perfusion of tumor (14, 15), which have been applied in the diagnosis of cervical cancer and the evaluation of response to radiotherapy and chemotherapy (16–18). Previous studies have also shown their potential in the preoperative evaluation of PLNM in cervical cancer (19). But the changing trend of quantitative parameters of these two technologies in different lymph node status is not clear, and there is still controversy over whether they can effectively predict PLNM (20, 21). Correctly understanding the microenvironment reflected by various functional parameters and exploring the relationship between microenvironmental abnormalities and tumor invasiveness in depth is beneficial for accurately evaluating whether corresponding MR techniques can serve as reliable tools for predicting PLNM.

SCC-Ag is the most commonly used serum tumor marker for monitoring cervical cancer. Previous studies have shown that the elevated SCC-Ag before treatment are positively correlated with the risk of lymph node metastasis. However, the predictive value of SCC-Ag alone as a standard for PLNM is still insufficient, its diagnostic accuracy can be improved when combined with imaging examinations (22, 23). Therefore, we aimed to explore the value of combining quantitative parameters derived from IVIM-DWI and DCE-MRI of primary tumor with SCC-Ag in predicting PLNM for ECC patients.

Materials and methods

Patients

This study was approved by the Ethics Committee of our hospital and informed consent was waived. Medical records of patients diagnosed with FIGO IB~IIA cervical cancer from April 2022 to August 2023 were retrospectively analyzed. Inclusion criteria: (1) Pelvic MRI examination was performed within 2 weeks before surgery, include IVIM-DWI and DCE-MRI; (2) Radical hysterectomy combined with pelvic lymphadenectomy was performed, and confirmed cervical cancer histologically; (3) clinical and pathological data were complete. Exclusion criteria: (1) The histological type is not squamous cell carcinoma; (2) Accompanied by acute pelvic inflammatory response or other malignant tumors; (3) The image quality is unqualified due to the presence of artifacts,such as motion artifact; (4) The diameter of the tumor is less than 1cm, which affects the ROI outlining and the effective analysis of data; (4) Received preoperative chemotherapy or conization. According to the inclusion and exclusion criteria, 115 cases were ultimately selected and divided into PLNM group and non-PLNM group based on pathologic results (Figure 1). Clinical data of all patients including age, menstrual status, pregnancy, parturition, and abortion numbers, and FIGO stage were recorded. Peripheral venous blood was collected in a fasting state within one week before the patients received treatment, and serum SCC-Ag levels were measured by electrochemiluminescence.

MRI acquisition

The MRI scan was performed on a 3.0 T scanner (Discovery MR750W, GEHC, Waukesha, WI, USA) with a 16-channel body coil. To prevent intestinal peristalsis, an intramuscular injection of 10 mg of scopolamine hydrochloride was given 20 minutes before the examination. Order the patients to properly empty their bladder to minimize urine electrolyte artifact. MRI scan sequences include: (1) Axial fat-suppressed T2-weighted image (TR:9091ms, TE:98ms, FOV:420mm×420mm, NEX:2, slice thickness:7mm, slice spacing:1mm); (2) Oblique axial and coronal T2-weighted image (perpendicular and parallel to the long diameter of the tumor, respectively, TR:3532ms, TE:102ms, FOV:200mm×200mm, NEX:4, slice thickness:3mm, slice spacing:0.5mm); (3) Axial T1-weighted image (TR:786ms, FOV:420mm×420mm, NEX:1, slice thickness:7mm, slice spacing:1mm);(4) IVIM-DWI (Using a single-shot diffusion-weighted spin-echo planar sequence, 11 b-values were 0, 20, 50, 80, 100, 200, 400, 600, 800, 1000, 1500 s/mm^2), NEX were 1, 1, 1, 1, 1, 2, 2, 3, 4, 6, 8, TR:2084ms, TE:minimum, FOV:380mm×380mm, slice thickness:5mm, slice spacing:1 mm; (5) DCE-MRI (Using 3D-LAVA Flex sequence, TR:4.3ms, TE:2ms, NEX:1, FOV 400mm×400mm, slice thickness:4 mm, slice spacing: 0 mm, 40 phase of uninterrupted scanning was performed in the free-breathing state, with a single phase scanning time of 9s. Gd-DTPA was injected through the elbow vein at a flow rate of 3.5 mL/s at a dose of 0.1 mmol/kg from the beginning of the second phase, followed by a 15-mL saline flush of at the same rate.

Image analysis

The MRI original images were imported into GE AW 4.7 workstation. Image analysis and parameter measurements were double-blindly performed by two radiologists with more than 3 years of experience in the diagnosis of pelvic magnetic resonance imaging. The region of interest (ROI) was manually drawn around the lesion edge at the largest level of the tumor in the images of functional MRI sequences, exclude hemorrhage, necrosis, cystic degeneration, and the cervical canal, referenced to axial fat-suppressed T2WI. The volume transfer constant (K^{trans}), rate constant (K_{ep}), and extravascular extracellular volume fraction (V_e) were obtained from post-processed images of DCE-MRI images using the Gen IQ software. The apparent diffusion coefficient (ADC_{mean}, ADC_{min}, ADC_{max}), diffusion coefficient (D), pseudo diffusion coefficient (D*), and perfusion fraction (f) were generated by Functool software postprocessing of IVIM-DWI images. Images of typical cases are shown in Figure 2 and Figure 3.

Surgery and pathology

All the patients underwent radical hysterectomy and pelvic lymphadenectomy. Pelvic lymph node dissection included common iliac, internal iliac, external iliac, and obturator fossa lymph nodes of two sides. The surgical specimen were processed according to standard pathology procedures. Two pathologists with more than 3 years of diagnostic experience read the tissue sections to determine and record the depth of invasion, lymph-vascular space invasion (LVSI), and differentiation. The two physicians consult to determine the final conclusion in case of disagreement. All the dissected pelvic lymph nodes were numbered, stained with hematoxylin-hematoxylin-eosin staining supplemented with immunohistochemistry to determine benign and malignant by pathologists. PLNM was defined as the presence of metastasis in any one or more of the resected lymph nodes, and all cases were categorized into PLNM group and non-PLNM group based on the pathologic findings.

Statistical analysis

Statistical analysis of clinical and imaging data was performed using SPSS 26.0 software. The interobserver agreement all parameters

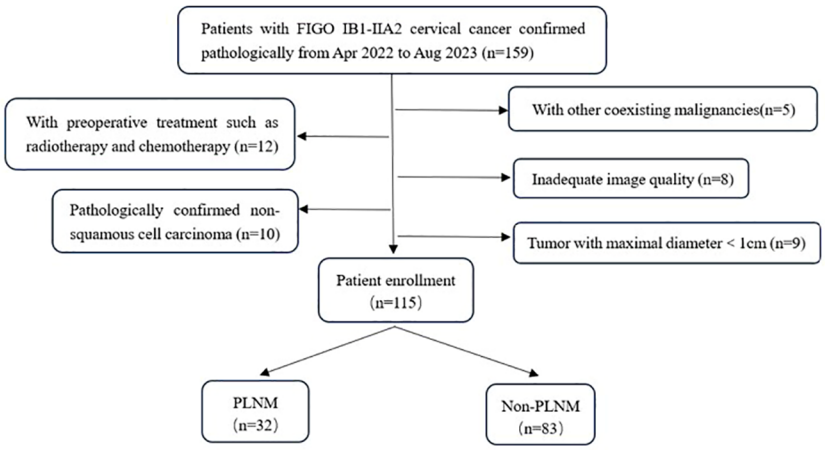

FIGURE 1
Flowchart of patient enrollment.

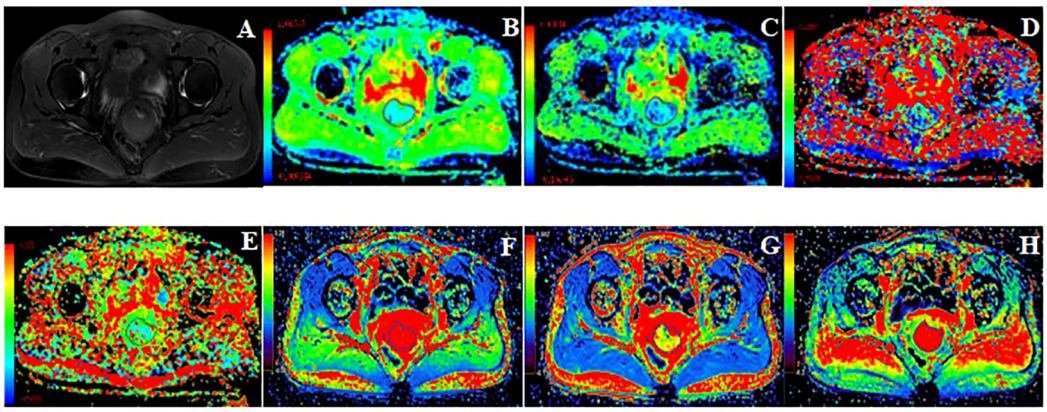

FIGURE 2
49 years old, FIGO IB3 cervical cancer with PLNM. **(A)**: Axial T2WI image, **(B–H)**: Pseudo-color images of each quantitative parameter of DCE-MRI and IVIM-DWI, **(B)**: ADC_{min} was $0.47\times10^{-3}mm^2/s$, ADC_{mean} was $0.61\times10^{-3}mm^2/s$, ADC_{max} was $0.85\times10^{-3}mm^2/s$ **(C)**: D was $0.49\times10^{-3}mm^2/s$, **(D)**: D* was $30.50\times10^{-3}mm^2/s$, **(E)**: f was 0.12, **(F)**: Ktrans was 0.49 min^{-1}, **(G)**: V_e was 0.27, **(H)**: K_{ep} was 1.79 min^{-1}.

were assessed using the intraclass correlation coefficient (ICC), with ICC >0.75 indicating high consistency. The normality of quantitative data was determined by Shapiro-Wilk test. The above normally distributed data was compared using student t-test and described as mean ± standard deviation. Non-normally distributed data was compared using the Mann-Whitney U test a described as median with inter-quartile range (IQR). Comparisons of counting data was conducted by chi-square or Fisher's exact tests. Statistically significant parameters in the above univariate analysis were jointly included in multivariate Logistic regression analysis to determine the risk factors for PLNM. Receiver operating characteristic (ROC) curve was used to assess the diagnostic efficacy of individual parameters and their combination in predicting PLNM from ECC. *P*-value < 0.05 was considered statistically significant.

Results

Clinicopathologic characteristics

A total of 115 patients were enrolled, with different cervical cancer stages including 23 cases of IB1, 24 cases of IB2, 13 cases of IB3, 21 cases of IIA1, and 34 cases of IIA2, with a mean age of 55.77 ± 10.03 (ranged from 31 to 81) years. There was no significant difference between the PLNM group and the non-PLNM group in age, menstrual status, pregnancy, parturition, and abortion numbers, and degree of differentiation (P > 0.05). Statistically significant difference in FIGO stage, depth of infiltration, LVSI, and SCC-Ag (P < 0.001). The clinicopathologic data were shown in Table 1.

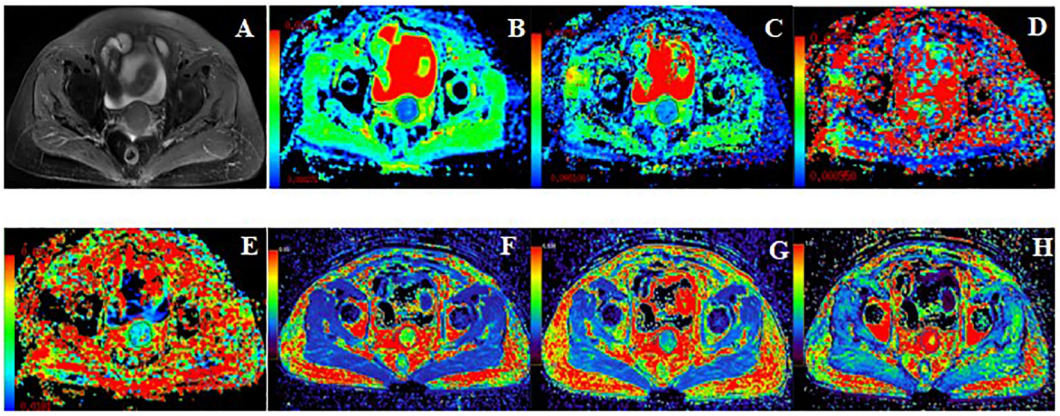

FIGURE 3
62 years old, FIGO IIA2 cervical cancer without PLNM. **(A)**: Axial T2WI image. **(B–H)**: Pseudo-color images of each quantitative parameter of DCE-MRI and IVIM-DWI, **(A)**: Axial T2WI image, **(B)**: ADC_{min} was $0.67\times10^{-3}mm^2/s$, ADC_{mean} was $0.77\times10^{-3}mm^2/s$, ADC_{max} was $1.10\times10^{-3}mm^2/s$ **(C)**: D was $0.61\times10^{-3}mm^2/s$, **(D)**: D* was $30.00\times10^{-3}mm^2/s$, **(E)**: f was 0.15, **(F)**: K^{trans} was 1.19 min^{-1}, **(G)**: V_e was 0.35, **(H)**: K_{ep} was 3.56 min^{-1}.

Comparison of DCE-MRI and IVIM-DWI quantitative parameters of the primary tumor

The consistency test of inter-observer measurements present high reproducibility. The ICC (95% CI) of all parameters were listed in Table 2. The PLNM group presented lower K^{trans} (0.51 ± 0.20 min^{-1} vs.0.80 ± 0.33 min^{-1}, $P < 0.001$), ADC_{mean} (0.85 ± 0.09 mm/s^2 vs.1.06 ± 0.35 mm/s^2, $P<0.001$), ADC_{min} [0.67 (0.61,0.75) mm/s^2 vs. 0.75 (0.64,0.90) mm/s^2, $P = 0.012$] and f (0.91 ± 0.09 vs. 0.27 ± 0.14, $P = 0.001$) than the non-LNM group. There was no statistically significant difference of K_{ep}, V_e, D and D* between the two groups ($P > 0.05$). Comparisons of parameters are shown in Table 3.

Multivariate logistic regression analysis to determine independent risk factors

Parameters with statistically significant differences in Univariate analysis (K^{trans}, ADC_{mean}, ADC_{min}, ADC_{max}, f, and SCC-Ag) were included in the multivariate Logistic regression analysis, and showed that SCC-Ag (OR=1.154, $P < 0.05$), K^{trans} (OR=0.003, $P < 0.001$) and f (OR=0.001, $P < 0.05$) were independent risk factors of PLNM. Multivariate Logistic regression analysis of parameters was shown in Table 4.

Diagnostic efficacy of K^{trans}, f, SCC-Ag and their combination for predicting PLNM

ROC analysis of K^{trans}, f, SCC-Ag and their combination in predicting PLNM is shown in Table 5 and Figure 4. The area under curve (AUC) of SCC-Ag, K^{trans}, and f for predicting PLNM were 0.824, 0.797 and 0.793, respectively. And the combination of those three parameters yields the highest diagnostic efficacy with the AUC of 0.896. The sensitivity and specificity are 79.1% and 94.0%, respectively, with the prediction accuracy of 87%.

TABLE 1 Comparison of clinical and pathological data in two groups.

Characteristics	PLNM (n=32)	Non-PLNM(n=83)	$t/\chi^2/Z$	*P*
Age(years)	57.56 ± 11.13	55.08 ± 9.56	-1.189	0.237
FIGO stage(n)			29.26	<0.001
IB1	0	23		
IB2	3	21		
IB3	2	11		
IIA1	7	14		
IIA2	20	14		
Menopausal status(n)			0.047	0.829
Menstruation	11	28		
Menopause	20	56		
Pregnancy numbers(n)	3.16 ± 1.51	3.47 ± 1.32	-1.098	0.274
Parturition numbers(n)	2.00 ± 1.02	2.27 ± 0.89	-1.381	0.170
Abortion numbers(n)	1.16 ± 0.89	1.20 ± 1.12	-0.244	0.808
Depth of invasion(n)			16.321	<0.001
≥2/3 of cervical wall	25	30		
<2/3 of cervical wall	7	53		
Histologic grade(n)			1.495	0.473
Low grade	10	35		
Middle grade	17	14		
High grade	15	14		
LVSI(n)			30.218	<0.001
Yes	23	15		
No	9	68		
SCC-Ag(ng/ml)	14.25(6.74,36.75)	2.13(1.32,6.00)	-5.374	<0.001

PLNM, pelvic lymph node metastasis, LVSI, lymph-vascular space invasion, SCC-Ag, squamous cell carcinoma antigen.

Discussion

PLNM is closely related to the poor prognosis of ECC, and accurate preoperative assessment of pelvic lymph node status can help some patients to avoid nonessential pelvic lymph node dissection and make a decision of whether to choose surgery or radiotherapy as the primary treatment. There were 115 patients with FIGO stage IB1-IIA2 cervical cancer included, 32 with PLNM, accounting for approximately 27.8%, which is similar to the previously reported incidence of PLNM in ECC patients (24). In this study, we investigated the application value of IVIM-DWI and DCE-MRI for predicting PLNM, and further explored the combined diagnostic efficacy of the above functional techniques and preoperative serum SCC-Ag for PLNM.

DCE-MRI is a non-invasive perfusion imaging technique that can evaluate the lesion microcirculation and capillary permeability by quantifying the contrast exchange information between tumor vascular and extracellular interstitial space, and calculating several perfusion parameters using mathematical models (20). Among them, K^{trans} reflects the flow rate of contrast agent from the vessel to the interstitial space, K_{ep} reflects contrast agent reflux rate from the interstitial space to the capillary, and V_e is defined as the volume fraction occupied by the extravascular-extracellular space. The first two parameters depend on microvascular permeability, surface area and blood flow, While V_e reflects the degree of cell necrosis and proliferation (25).

Our study demonstrated that K^{trans} was significantly lower in the PLNM group than in the non-PLNM group, suggesting a relative decreased microvascular permeability in the primary lesion, and a similar finding was also reported in an animal experimental study by KIRSTI et al. (26). Several other studies

TABLE 2 Consistency test of the quantitative parameters measured by two observers.

Paremeters	Intraclass correlation coefficient	95% confidence interval
K^{trans}	0.810	0.735-0.865
V_e	0.767	0.679-0.833
K_{ep}	0.872	0.820-0.910
ADC_{mean}	0.834	0.767-0.882
ADC_{min}	0.854	0.795-0.896
ADC_{max}	0.753	0.662-0.823
D	0.789	0.709-0.849
D*	0.929	0.899-0.951
f	0.754	0.662-0.823

have shown that DCE-MRI can be used to characterize unfavorable microenvironments such as hypoxia (27, 28), and that K^{trans} is the most robust and sensitive parameter for assessing HIF-1α expression, which is significantly reduced in hypoxic tumor cells (29). Thus, the correlation between changes in K^{trans} of primary tumors and metastatic tendency may reflect an underlying mechanism by which lymphatic spread is driven by hypoxia. Due to the complex and disorganized process of tumor angiogenesis, it often leads to microvascular structural abnormalities and dysfunction, which results in decreased blood transit to the interstitial space space, inadequate supply of oxygen, glucose, and other nutrients, and up-regulation of lymphangiogenic factors to promote PLNM (30).

Bai et al. (31) demonstrated that K_{ep} of primary tumor could be used to predict PLNM. High interstitial fluid pressure promotes

TABLE 3 Comparison of DCE-MRI and IVIM-DWI parameters in two groups.

Paremeters	PLNM (n=32)	Non-PLNM(n=83)	*t/Z*	*P*
DCE-MRI				
K^{trans}	0.51 (0.20)	0.80(0.33)	5.556	<0.001
K_{ep}	1.34(1.10,1.64)	1.30(0.83,1.83)	−0.524	0.600
V_e	0.42(0.35,0.48)	0.49(0.35,0.74)	−1.888	0.059
IVIM-DWI				
ADC_{mean}	0.85(0.09)	1.06(0.35)	5.127	<0.001
ADC_{min}	0.67(0.61,0.75)	0.75(0.64,0.90)	−2.515	0.012
ADC_{max}	1.22(0.28)	1.42(0.40)	3.100	0.003
D	0.69(0.61,0.74)	0.70(0.52,0.88)	−0.512	0.609
D*	33.55(22.08,50.65)	37.00(18.60,54.20)	−0.403	0.687
f	0.19(0.09)	0.27(0.14)	3.499	0.001

PLNM, pelvic lymph node metastasis, DCE-MRI, dynamic contrast-enhanced magnetic resonance imaging, IVIM-DWI, intravoxel incoherent motion diffusion-weighted imaging.

TABLE 4 Independent risk factors analysis of PLNM.

Paremeters	Odds Ratio	Wald	*P*
SCC-Ag	1.054	7.339	0.007
K^{trans}	0.003	14.559	<0.001
ADC_{mean}	0.224	0.083	0.773
ADC_{min}	0.384	0.053	0.818
ADC_{max}	0.247	0.935	0.334
f	0.001	4.394	0.036

SCC-Ag, squamous cell carcinoma antigen.

reflux. At the same time, tumor interstitial fluid carrying undesirable factors such as lymphangiogenesis factors enters normal tissue. Thus, higher K_{ep} increases the risk of PLNM. Our study also showed a trend of higher Kep of primary tumors in the PLNM group, but there is no statistically significant difference between groups. This may be related to the difference in the proportion of different stages of the cases included in the study. In addition, our study found that the V_e of primary tumors in the PLNM group was lower than that in the non-PLNM group, suggesting that the abnormal proliferation of tumor cells resulted in reduced interstitial space. This is consistent with the high pressure of interstitial fluid reflected by high K_{ep} and the relative decrease in perfusion reflected by low K^{trans}, but the difference in V_e between groups was also not statistically significant. Previous studies have shown that changes in V_e are the result of a combination of cell proliferation and micronecrosis (32). Even though necrotic regions were avoided when outlining ROIs, the effect of micro-necrosis could not be excluded. Therefore, V_e tends to be unstable in reflecting the state of tumor microenvironment and aggressiveness.

IVIM-DWI can realize the separation and quantitative evaluation of water molecule diffusion and microcirculation perfusion by setting up three or more b -values. It compensates the limitations in diffusion accuracy of single b-value DWI (33, 34).

In this study, the IVIM-DWI quantitative parameters of primary tumors in the PLNM group were lower than those in the no-PLNM group, with statistically significant differences between groups in ADC and f values. Abnormal cell proliferation in highly aggressive tumors leads to a narrowing of the extracellular space and lower ADC values, which is consistent with the results of most previous studies (35–37). f represents the volume ratio of the diffusion effect of microcirculatory perfusion within the voxel to the overall diffusion effect. Pathologically, cell proliferation in malignant tumors is dependent on neovascularization, and therefore blood perfusion is increased accordingly. However, we found that the f was lower in the PLNM group than that in the non-PLNM group, which is contrary to the above theory. Jose et al. (38) also reported the similar findings. We suspected that f will change with lesion progression. In the early stage of cervical cancer, blood supply demand increases and f rises with the increase in microvessel density. However, with sufficient oxygen and nutrients provided by neovascularization, tumor proliferation accelerates and increases in size, while cancer cells can invade the vasculature and increase fluid

TABLE 5 Diagnostic efficiency of K^{trans}, f, ADC and their combination.

Variable	AUC	Cut off	Sensitivity	Specificity	Accuracy
SCC-Ag	0.824	3.14	0.938	0.639	0.77
f	0.703	0.17	0.531	0.771	0.72
K^{trans}	0.797	0.59	0.719	0.771	0.79
Combination	0.896	0.44	0.791	0.940	0.87

SCC-Ag, squamous cell carcinoma antigen. AUC, area under the curve.

viscosity (39), leading to poor perfusion and lower f. Therefore, the microenvironment of lesions is a dynamic evolutionary process. Subgrouping based on different FIGO stages or tumor volumes to explore the pathological features of cervical cancer in detail can help to clarify the real microcirculatory status of each stage of the lesion. Besides, our study found that K^{trans}, which reflects microvascular permeability, and f, which reflects capillary density, both showed a decreasing trend in the PLNM group, and the perfusion characteristics of the lesions reflected by the two were consistent. Moreover, in a previous study exploring the differentiation degree of cervical cancer, M et al. found there is a correlation between f and the quantitative and semi quantitative parameters of DCE-MRI, with a moderate correlation between f and K^{trans}. This suggests that IVIM-DWI can provide an alternative perfusion imaging method for patients with renal dysfunction (13).

D and D* of primary tumors in the PLNM group in our study tended to decrease, but none of the differences between the groups were statistically significant. D is an important indicator of cell density and extracellular space, which is negatively correlated with cell density and nucleus/cytoplasm ratio (33), and the ability of D to reflect PLNM may depend on the cellular denseness of a local area rather than of the whole lesion (14), therefore, it is closely related to the scope and accuracy of ROI outlining. D* represents diffusion information caused by capillary perfusion, which correlates with local blood flow. Although D* also reflects perfusion characteristics, studies have shown that it is not as reproducible as f (40). The stability of IVIM-DWI parameter measurements is also affected by the b-value. The stability and consistency of the parameters with different combinations of b-values, as well as the selection of optimal b-values, need to be further explored.

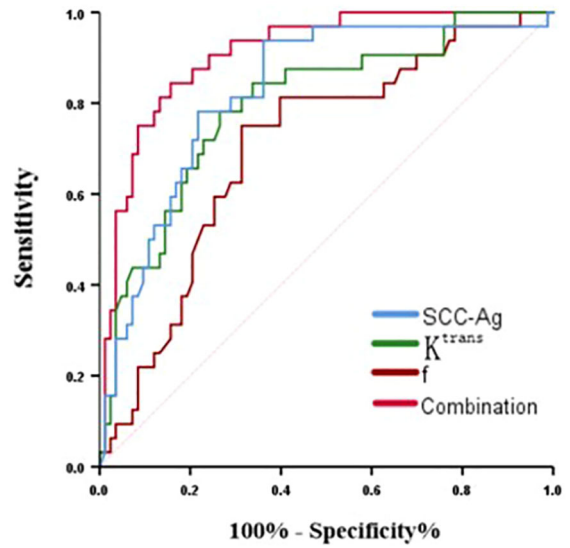

FIGURE 4
ROC curve of K^{trans}, f, ADC and their combination for predicting PLNM in cervical cancer.

SCC-Ag is a relatively specific tumor marker for cervical squamous carcinoma. With the proliferation and spread of cancer cells, a large amount of SCC-Ag is produced and released into the blood. Its level is closely related to tumor cell activity and tumor load (41). Consistent with previous reports (42), our study also found that higher SCC-Ag was significantly associated with PLNM in ECC, and its diagnostic efficacy in predicting PLNM (AUC=0.824) was even higher than the K^{trans} and f, suggesting that it can be used as a convenient marker for clinical adjuvant assessment of PLNM.

Considering that a single parameter may be affected by multiple factors and cannot fully and accurately reflect lesion characteristics, we explored the value of the combination of K^{trans}, f-value and SCC-Ag in diagnosing PLNM and found it yielded the highest AUC of 0.896. The combined prediction represents a comprehensive analysis of tumor-specific antigen expression levels and lesion microcirculation perfusion characteristics. Therefore, its diagnostic efficacy is superior to that of each single parameter, suggesting that the combined application of multiparametric MRI and tumor markers provide a more comprehensive evaluation of tumor aggressiveness, which may further improve the accuracy of predicting PLNM.

There are several limitations in our study. First, to ensure the feasibility and accuracy of ROI outlining, cases with lesion diameters less than 1 cm were excluded, which may lead to bias in the overall results. Second, only cervical squamous carcinoma cases were included in this study, and whether the conclusion is applicable to other histologic types such as adenocarcinoma needs to be explored. In addition, due to the small sample size, the changes in tumor parameters of different FIGO stages were not further analyzed.

Conclusion

In conclusion, quantitative parameters K^{trans} and f of primary tumors and preoperative serum SCC-Ag in have certain predictive value for PLNM in ECC, and their combination further improves the diagnostic efficacy, which is helpful to provide imaging guidance

for clinicians to design the optimal treatment plan for cervical cancer patients.

Data availability statement

The original contributions presented in the study are included in the article/supplementary material. Further inquiries can be directed to the corresponding author.

Ethics statement

The studies involving humans were approved by Ethics Committee of CangZhou Central Hospital. The studies were conducted in accordance with the local legislation and institutional requirements. The ethics committee/institutional review board waived the requirement of written informed consent for participation from the participants or the participants' legal guardians/next of kin because 1) It is a retrospective study with minimal risk to participants. 2) No adverse impact on participants' rights and health. 3) Important value of the study. 4) Privacy and confidentiality were protected.

Author contributions

XX: Data curation, Investigation, Methodology, Writing – original draft. FL: Supervision, Writing – review & editing. XRZ: Methodology, Writing – review & editing. CW: Methodology, Writing – review & editing. DL: Methodology, Writing – review & editing. LK: Conceptualization, Project administration, Supervision, Writing – review & editing. SL: Validation, Writing – review & editing. XLZ: Validation, Writing – review & editing.

Funding

The author(s) declare that no financial support was received for the research, authorship, and/or publication of this article.

Conflict of interest

The authors declare that the research was conducted in the absence of any commercial or financial relationships that could be construed as a potential conflict of interest.

Publisher's note

References

1. Sung H, Ferlay J, Siegel RL, Laversanne M, Soerjomataram I, Jemal A, et al. Global cancer statistics 2020: globocan estimates of incidence and mortality worldwide for 36 cancers in 185 countries. *CA Cancer J Clin.* (2021) 71:209–49. doi: 10.3322/Caac.21660

2. Guo Q, Zhu J, Wu Y, Wen H, Xia L, Ju X, et al. Validation of the prognostic value of various lymph node staging systems for cervical squamous cell carcinoma following radical surgery: A single-center analysis of 3,732 patients. *Ann Transl Med.* (2020) 8:485. doi: 10.21037/Atm.2020.03.27

3. Gien LT, Covens A. Lymph node assessment in cervical cancer: prognostic and therapeutic implications. *J Surg Oncol.* (2009) 99:242–7. doi: 10.1002/Jso.21199

4. Greggi S, Scaffa C. Surgical management of early cervical cancer: the shape of future studies. *Curr Oncol Rep.* (2012) 14:527–34. doi: 10.1007/S11912-012-0269-1

5. Bhatla N, Berek JS, Cuello Fredes M, Denny LA, Grenman S, Karunaratne K, et al. Revised figo staging for carcinoma of the cervix uteri. *Int J Gynaecol and Obstetrics: Off Organ Int Fed Gynaecol and Obstetrics.* (2019) 145:129–35. doi: 10.1002/Ijgo.12749

6. Li X, Yin Y, Sheng X, Han X, Sun L, Lu C, et al. Distribution pattern of lymph node metastases and its implication in individualized radiotherapeutic clinical target volume delineation of regional lymph nodes in patients with stage IA to IIA cervical cancer. *Radiat Oncol.* (2015) 10:40. doi: 10.1186/S13014-015-0352-5

7. Marth C, Landoni F, Mahner S, Mccormack M, Gonzalez-Martin A, Colombo N. Cervical cancer: esmo clinical practice guidelines for diagnosis, treatment and follow-up. *Ann Oncol: Off J Eur Soc For Med Oncol.* (2017) 28:Iv72–83. doi: 10.1093/Annonc/Mdx220

8. Wenzel HHB, Olthof EP, Bekkers RLM, Boere IA, Lemmens V, Nijman HW, et al. Primary or adjuvant chemoradiotherapy for cervical cancer with intraoperative lymph node metastasis - A review. *Cancer Treat Rev.* (2022) 102:102311. doi: 10.1016/J.Ctrv.2021.102311

9. Xiao M, Yan B, Li Y, Lu J, Qiang J. Diagnostic performance of mr imaging in evaluating prognostic factors in patients with cervical cancer: A meta-analysis. *Eur Radiol.* (2020) 30:1405–18. doi: 10.1007/S00330-019-06461-9

10. Meng H, Guo X, Zhang D. Multimodal magnetic resonance imaging in the diagnosis of cervical cancer and its correlation with the differentiation process of cervical cancer. *BMC Med Imaging.* (2023) 23:144. doi: 10.1186/S12880-023-01104-4

11. Olthof EP, van der Aa MA, Adam JA, Stalpers LJA, Wenzel H, van der Velden J, et al. The role of lymph nodes in cervical cancer: incidence and identification of lymph node metastases-A literature review. *Int J Clin Oncol.* (2021) 26:1600–10. doi: 10.1007/S10147-021-01980-2

12. Shen G, Zhou H, Jia Z, Deng H. Diagnostic performance of diffusion-weighted mri for detection of pelvic metastatic lymph nodes in patients with cervical cancer: A systematic review and meta-analysis. *Br J Radiol.* (2015) 88:20150063. doi: 10.1259/Bjr.20150063

13. Wang H, Zhu L, Li G, Zuo M, Ma X, Wang J. Perfusion parameters of intravoxel incoherent motion based on tumor edge region of interest in cervical cancer: evaluation of differentiation and correlation with dynamic contrast-enhanced mri. *Acta Radiol (Stockholm Sweden: 1987).* (2020) 61:1087–95. doi: 10.1177/0284185119890086

14. Mi HL, Suo ST, Cheng JJ, Yin X, Zhu L, Dong SJ, et al. The invasion status of lymphovascular space and lymph nodes in cervical cancer assessed by mono-exponential and bi-exponential dwi-related parameters. *Clin Radiol.* (2020) 75:763–71. doi: 10.1016/J.Crad.2020.05.024

15. Ellingsen C, Walenta S, Hompland T, Mueller-Klieser W, Rofstad EK. The microenvironment of cervical carcinoma xenografts: associations with lymph node metastasis and its assessment by dce-mri. *Trans Oncol.* (2013) 6:607–17. doi: 10.1593/Tlo.13313

16. Matani H, Patel AK, Horne ZD, Beriwal S. Utilization of functional mri in the diagnosis and management of cervical cancer. *Front Oncol.* (2022) 12:1030967. doi: 10.3389/Fonc.2022.1030967

17. Zheng X, Guo W, Dong J, Qian L. Prediction of early response to concurrent chemoradiotherapy in cervical cancer: value of multi-parameter mri combined with clinical prognostic factors. *Magn Reson Imaging.* (2020) 72:159–66. doi: 10.1016/J.Mri.2020.06.014

18. Qin F, Pang H, Ma J, Zhao M, Jiang X, Tong R, et al. Combined dynamic contrast enhanced mri parameter with clinical factors predict the survival of concurrent chemo-radiotherapy in patients with 2018 figo iiicr stage cervical cancer. *Eur J Radiol*. (2021) 141:109787. doi: 10.1016/J.Ejrad.2021.109787

19. Dappa E, Elger T, Hasenburg A, Düber C, Battista MJ, Hötker AM. The value of advanced mri techniques in the assessment of cervical cancer: A review. *Insights Into Imaging*. (2017) 8:471–81. doi: 10.1007/S13244-017-0567-0

20. Xu J, Ma Y, Mei H, Wang Q. Diagnostic value of multimodal magnetic resonance imaging in discriminating between metastatic and non-metastatic pelvic lymph nodes in cervical cancer. *Int J Gen Med*. (2022) 15:6279–88. doi: 10.2147/Ijgm.S372154

21. Zhang Y, Zhang KY, Jia HD, Fang X, Lin TT, Wei C, et al. Feasibility of predicting pelvic lymph node metastasis based on ivim-dwi and texture parameters of the primary lesion and lymph nodes in patients with cervical cancer. *Acad Radiol*. (2022) 29:1048–57. doi: 10.1016/J.Acra.2021.08.026

22. Zhou Z, Li W, Zhang F, Hu K. The value of squamous cell carcinoma antigen (Scca) to determine the lymph nodal metastasis in cervical cancer: A meta-analysis and literature review. *PloS One*. (2017) 12:E0186165. doi: 10.1371/Journal.Pone.0186165

23. Xu D, Wang D, Wang S, Tian Y, Long Z, Ren X. Correlation between squamous cell carcinoma antigen level and the clinicopathological features of early-stage cervical squamous cell carcinoma and the predictive value of squamous cell carcinoma antigen combined with computed tomography scan for lymph node metastasis. *Int J Gynecol Cancer*. (2017) 27:1935–42. doi: 10.1097/Igc.0000000000001112

24. Zhang Z, Wan X, Lei X, Wu Y, Zhang J, Ai Y, et al. Intra- and peri-tumoral mri radiomics features for preoperative lymph node metastasis prediction in early-stage cervical cancer. *Insights Into Imaging*. (2023) 14:65. doi: 10.1186/S13244-023-01405-W

25. Alareer HSN, Jasim Taher H, Dinar Abdullah A. Dynamic contrast enhanced-mri and apparent diffusion coefficient quantitation for differentiate hepatocellular carcinoma from hepatocellular adenoma. *Asian Pacific J Cancer Prevention: Apjcp*. (2024) 25:931–7. doi: 10.31557/Apjcp.2024.25.3.931

26. Øvrebø KM, Gulliksrud K, Mathiesen B, Rofstad EK. Assessment of tumor radioresponsiveness and metastatic potential by dynamic contrast-enhanced magnetic resonance imaging. *Int J Radiat Oncol Biol Phys*. (2011) 81:255–61. doi: 10.1016/J.Ijrobp.2011.04.008

27. Hillestad T, Hompland T, Fjeldbo CS, Skingen VE, Salberg UB, Aarnes EK, et al. Mri distinguishes tumor hypoxia levels of different prognostic and biological significance in cervical cancer. *Cancer Res*. (2020) 80:3993–4003. doi: 10.1158/0008-5472.Can-20-0950

28. Hauge A, Wegner CS, Gaustad JV, Simonsen TG, Andersen LMK, Rofstad EK. Dce-mri of patient-derived xenograft models of uterine cervix carcinoma: associations with parameters of the tumor microenvironment. *J Trans Med*. (2017) 15:225. doi: 10.1186/S12967-017-1331-4

29. Li X, Wu S, Li D, Yu T, Zhu H, Song Y, et al. Intravoxel incoherent motion combined with dynamic contrast-enhanced perfusion mri of early cervical carcinoma: correlations between multimodal parameters and hif-1α Expression. *J Magn Reson Imaging*. (2019) 50:918–29. doi: 10.1002/Jmri.26604

30. Wong BW. Lymphatic vessels in solid organ transplantation and immunobiology. *Am J Transplantation: Off J Am Soc Transplant and Am Soc Transplant Surgeons*. (2020) 20:1992–2000. doi: 10.1111/Ajt.15806

31. Bai Z, Shi J, Yang Z, Zeng W, Hu H, Zhong J, et al. Quantitative kinetic parameters of primary tumor can be used to predict pelvic lymph node metastasis in early-stage cervical cancer. *Abdom Radiol (Ny)*. (2021) 46:1129–36. doi: 10.1007/S00261-020-02762-6

32. Zhang X, Dong Y, Song Q, Zhu Y, Pang H, Luo Y, et al. The role of multiparametric magnetic resonance imaging in the study of primary tumor and pelvic lymph node metastasis in stage ib1-iia1 cervical cancer. *J Comput Assist Tomogr*. (2020) 44:750–8. doi: 10.1097/Rct.0000000000001084

33. Song J, Lu Y, Wang X, Peng W, Lin W, Hou Z, et al. A comparative study of four diffusion-weighted imaging models in the diagnosis of cervical cancer. *Acta Radiol (Stockholm Sweden: 1987)*. (2022) 63:536–44. doi: 10.1177/02841851211002017

34. Ge YX, Hu SD, Wang Z, Guan RP, Zhou XY, Gao QZ, et al. Feasibility and reproducibility of T2 mapping and dwi for identifying Malignant lymph nodes in rectal cancer. *Eur Radiol*. (2021) 31:3347–54. doi: 10.1007/S00330-020-07359-7

35. Song Q, Yu Y, Zhang X, Zhu Y, Luo Y, Yu T, et al. Value of mri and diffusion-weighted imaging in diagnosing normal-sized pelvic lymph nodes metastases in patients with cervical cancer. *Br J Radiol*. (2022) 95:20200203. doi: 10.1259/Bjr.20200203

36. He XQ, Wei LN. Diagnostic value of lymph node metastasis by diffusion-weighted magnetic resonance imaging in cervical cancer. *J Cancer Res Ther*. (2016) 12:77–83. doi: 10.4103/0973-1482.148726

37. Wang Y, Chen X, Pu H, Yuan Y, Li S, Chen G, et al. Roles of dwi and T2-weighted mri volumetry in the evaluation of lymph node metastasis and lymphovascular invasion of stage ib-iia cervical cancer. *Clin Radiol*. (2022) 77:224–30. doi: 10.1016/J.Crad.2021.12.011

38. Perucho JAU, Chiu KWH, Wong EMF, Tse KY, Chu MMY, Chan LWC, et al. Diffusion-weighted magnetic resonance imaging of primary cervical cancer in the detection of sub-centimetre metastatic lymph nodes. *Cancer Imaging*. (2020) 20:27. doi: 10.1186/S40644-020-00303-4

39. Shi B, Dong JN, Zhang LX, Li CP, Gao F, Li NY, et al. A combination analysis of ivim-dwi biomarkers and T2wi-based texture features for tumor differentiation grade of cervical squamous cell carcinoma. *Contrast Media Mol Imaging*. (2022) 2022:2837905. doi: 10.1155/2022/2837905

40. Andreou A, Koh DM, Collins DJ, Blackledge M, Wallace T, Leach MO, et al. Measurement reproducibility of perfusion fraction and pseudodiffusion coefficient derived by intravoxel incoherent motion diffusion-weighted mr imaging in normal liver and metastases. *Eur Radiol*. (2013) 23:428–34. doi: 10.1007/S00330-012-2604-1

41. Salvatici M, Achilarre MT, Sandri MT, Boveri S, Vanna Z, Landoni F. Squamous cell carcinoma antigen (Scc-ag) during follow-up of cervical cancer patients: role in the early diagnosis of recurrence. *Gynecol Oncol*. (2016) 142:115–9. doi: 10.1016/J.Ygyno.2016.04.029

42. Xu F, Li Y, Fan L, Ma J, Yu L, Yi H, et al. Preoperative scc-ag and thrombocytosis as predictive markers for pelvic lymphatic metastasis of squamous cervical cancer in early figo stage. *J Cancer*. (2018) 9:1660–6. doi: 10.7150/Jca.24049